A computational model of bone-cell interactions taking into account bone specific surface

Ch. Lerebours[*,1], P.R. Buenzli[2], C.D.L. Thomas[3], J.G. Clement[3], P. Pivonka[1]

[1]Northwest Academic Centre, Australian Inst. Musculoskeletal Science, University of Melbourne, VIC 3021, Australia.
[2]School of Mathematical Sciences, Monash University, VIC 3800, Australia.
[3]Melbourne Dental School, University of Melbourne, 720 Swanston Street, VIC 3053, Australia.

*email: chloe.lerebours@unimelb.edu.au

Abstract

Bone cells are well-known to be regulated biochemically and biomechanically. The notion that the microscopic availability of bone surface affects bone remodelling is, however, less established. Bone-resorbing and bone-forming cells require a bone surface to attach to and initiate the matrix renewal. In this paper, we will extend a previous computational model of bone remodelling. This model includes several stages in the differentiation of bone cells, biochemical regulations and geometrical regulations. In particular a new calibration algorithm for uncommitted bone cells and activator/repressor functions is presented. This study is a necessary prerequisite to study endocortical bone loss due to aging in a spatio-temporal context.

Keywords: bone remodeling, specific surface, computational modeling, age-related bone loss

Introduction

Bone has several important roles: (i) keeping its integrity and sustaining the mechanical loading applied on it, (ii) a source/sink of calcium and phosphate regulating mineral homeostasis, and (iii) a protected space for haematopoiesis. Like in all other materials, loads that are applied on bone every day, lead to fatigue damage and micro cracks. Those cracks have to be repaired, otherwise they will grow and lead to macroscopic fracture. This is the role of the bone remodelling process, i.e., to resorb bone matrix containing cracks and to form new bone matrix thereafter. Three kinds of cells are responsible for the remodeling process: osteocytes (i.e., the mechanoreceptors, detect the cracks and activate remodelling); osteoclasts resorb the bone matrix and osteoblasts refill the hole. These cells are spatially and temporally organized in functional structures called BMUs - Basic Multicellular Units (Parfitt 1994).

Few computational models have been developed representing bone cell behaviours and more generally the remodelling process (Lemaire, Tobin et al. 2004); (Pivonka, Zimak et al. 2008); (Pivonka, Zimak et al. 2010); (Scheiner, Pivonka et al. 2013) (Buenzli, Thomas et al. 2013; Pivonka, Buenzli et al. 2013). They included biochemical, biomechanical and simplified geometrical regulations.

The aim of this paper is to develop a computational model of bone remodelling taking into account a comprehensive description of geometrical feedback. Emphasis is on the recalibration of uncommitted bone cells and the activator/repressor functions.

Materials and Methods

This paper is a continuation of our previous work on bone remodelling (Pivonka, Zimak et al. 2008; Pivonka, Buenzli et al. 2013) and, hence, only mathematical expressions relevant for explaining the underlying model behaviour are given below. For a complete list of equations and respective parameter values the reader is referred to previous publications and the CELLML model repository (see link in references). In the following we describe the essential features of the model.

Biochemical regulation

We modelled the interactions between osteoblasts and osteoclasts at various stages of differentiation using receptor-ligand binding reactions together with Hill-type functions (Figure 1); three stages in the differentiation of these bone cells are taken into account: uncommitted osteoclast and osteoblasts: OC_u and OB_u; osteoclast and –blast precursor cells: OC_p and OB_p and active cells: OC_a and OB_a. The uncommitted cells represent bone marrow stromal cells (OB_u) and hematopoietic stem cells (OC_u) respectively from which all other cells derive. Active osteoblasts (OB_a) produce bone matrix while active osteoclast (OC_a) resorb the bone matrix.
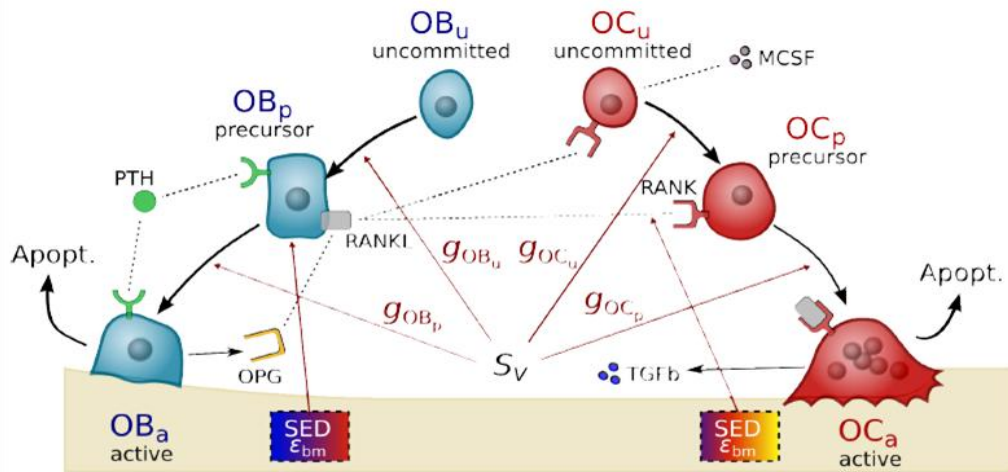

Figure 1 – Cell population model of bone remodeling including several developmental stages of osteoblasts and osteoclasts and their biochemical regulation, biomechanical regulation and geometrical regulation (Pivonka, Buenzli et al. 2013).

Communication between osteoblasts and osteoclasts enables a coordinated response to physiological demands, i.e., calcium and phosphate and the mechanical environment. Cells from the osteoclast lineage maintain a pool of osteoclast precursors through macrophage colony stimulation factor (MCSF, assumed constant) and RANKL (see next paragraph). Osteoclast precursor cells are then available for recruitment and differentiation into active osteoclasts.

Osteoblast lineage regulates the differentiation and the activity of osteoclasts. This pathway involves three major components: receptor activator of nuclear factor κβ: RANK, its ligand: RANKL and osteoprotegerin: OPG. RANK is expressed at the surface of uncommitted osteoclast and osteoclast precursor cells. RANKL is a polypeptide found at the surface of osteoblast precursor cells and can also be released as a soluble form (not modelled here). OPG is a decoy receptor molecule released by active osteoblastic cells. The differentiation of OCp into OCa requires binding of RANKL to RANK. The RANK - RANKL binding is inhibited by OPG which binds onto RANKL instead of RANK (Roodman 1999; Martin 2004). We sum up these interactions in the Figure 1.

Geometrical regulation

As pointed out in the introduction, there is increasing evidence that bone surface availability, i.e., bone specific surface, may play an important role in bone remodeling and particular in age-related bone loss. Bone cells are "working" on the surfaces of the bone matrix and consequently bone morphology plays an important role in the remodeling process. Osteoclasts require attachment to a surface to be able to resorb the bone matrix while osteoblasts only secrete osteoid on existing bone surfaces.

Two types of bone are usually distinguished, i.e., cortical and trabecular bone based on their respective porosity. Martin (Martin 1984) highlighted the differences between cortical and trabecular bones in terms of bone specific surface. In the cortical bone, an increase of porosity will increase the available surface, where remodeling can proceed, and so increase remodeling. However, in trabecular bone, increasing the porosity will decrease the available surface and decrease the remodeling (see Figure 2.a).
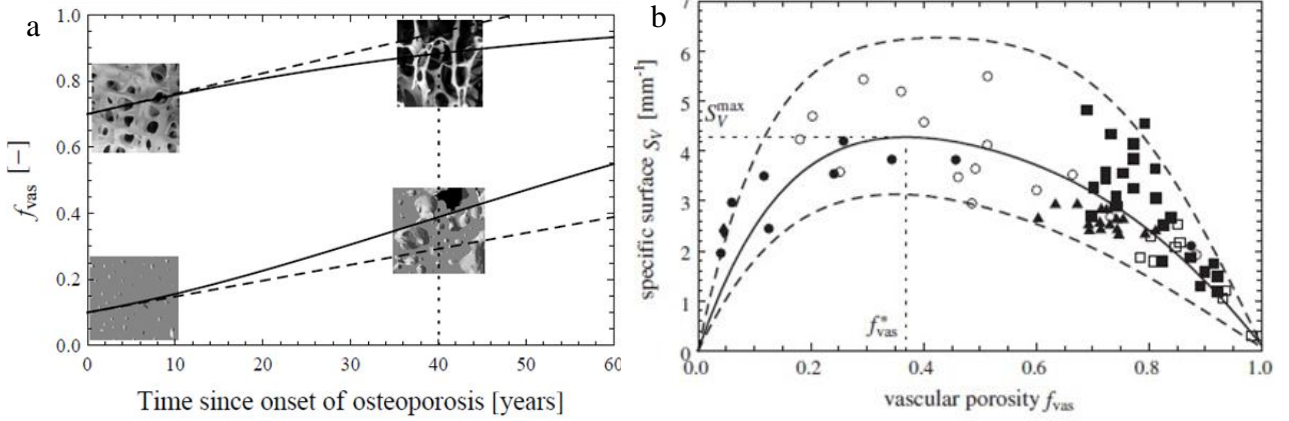

Figure 2 – a) Possible effect of geometrical feedback on the evolution of vascular porosity in osteoporosis, both in cortical and trabecular bone according to Martin (Martin 1972). Dashed curves show the changes in fvas obtained without geometrical feedback. b) Relation between bone specific surface and vascular porosity investigated by Martin (Martin 1984)

In order to introduce the effect of specific surface on bone cells we use a phenomenological function in the form of a polynomial similar as in (Pivonka, Buenzli et al. 2013):

$$g_i = \left(\frac{S_V}{S_{V\,t0}} \right)^{k_i} \; with \; S_V 0 = 1 \; mm^{-1} \tag{1}$$

where S_V is the specific surface; k_i is a constant determined based on a parametric study presented in the next section and "i" refers to the particular cell on which the regulatory function is applied. We note that unlike in the paper (Pivonka, Buenzli et al. 2013) $S_{V\,t0}$ is set equal to 1 leading to a dimensionless quantity. We believe that the original formulation, while suitable for the extreme cases of trabecular and cortical bone may have problems in properly describing the transition from cortical to trabecular bone. Hence, this new more consistent formulation has been used. We note that this formulation requires recalibration of the steady state values of the model (see discussion below).

The specific surface is based on B.R. Martin's equation (Martin 1984):

$$S_V(f_{vas}) = a.f_{vas} + b.f_{vas}^2 + c.f_{vas}^3 + d.f_{vas}^4 + e.f_{vas}^5 \tag{2}$$

where a, b, c, d and e are constants and f_{vas} is the vascular porosity in cortical bone and the marrow porosity in trabecular bone.

This relation has been obtained from interpolating of experimental data from an investigation on slices of cortical and trabecular bones both in humans and in animals. We are currently investigating the relationship between cortical porosity and bone specific surface using high resolution micro-CT in more detail in order to verify the accuracy of Eqn.(2). For the purpose of this paper we will base our theoretical developments on the porosity versus specific surface relationship provided by Martin, i.e., Eqn.(2) shown in Figure 2.b. (Martin 1984).

Unlike, in previous models, we believe that the OC_u and OB_u cell densities are not constant, but depend on the available pore space. Assuming that these densities should be related to the

3

respective pore space and to the observed remodeling rates we assume $OC_u = OC_u(f_{bm})$ and $OB_u = OB_u(f_{bm})$. Furthermore, we assume the shape of OC_u vascular density to follow a sigmoidal function. Indeed the vascular density is the density inside the pores. Hence, we assume the OC_u density to be higher where the porosity is low (i.e., $f_{bm} = 1$). Indeed, vascular pores in cortical bone are filled with blood vessels and BMUs. However, close to the marrow cavity, the trabecular pores are bigger but contain many other components such as bone marrow and fat. Hence, the density of bone cells in the vascular space is higher in cortical bone than in trabecular bone. Using suitable constraint conditions we then determine $OB_u(f_{bm})$ at homeostasis (i.e., the equilibrium state). More details are found below.

Bone cells equation
The evolution of bone cells is described mathematically based on "rate equations" (Lemaire, Tobin et al. 2004). The state variables are OB_p, OB_a, OC_p and OC_a, i.e., the cell densities. The Pi functions are Hill functions which represent the interaction – activation or repression – between a component (for example TGFβ) and a cell.

$$\frac{d\,OBp}{dt} = g_{OBu} * D_{OBu} * \pi_{act,OBu}^{TGF\beta} * OBu(fbm) + P_{OBp} * \pi_{act,OBp}^{mech} * OBp - D_{OBp} * \pi_{rep,OBp}^{TGF\beta} * OBp$$

$$\frac{dOBa}{dt} = D_{OBp} * \pi_{rep,OBp}^{TGF\beta} * OBp - (D_{OBa} + A_{OBa}) * OBa$$

$$\frac{dOCp}{dt} = g_{OCu} * D_{OCu} * \pi_{act,OCu}^{MCSF} * \pi_{act,OCu}^{RANKL} * OCu(fbm) - D_{OCp} * \pi_{act,OCp}^{RANKL} * OCp$$

$$\frac{dOCa}{dt} = D_{OCp} * \pi_{act,OCp}^{RANKL} * OCp - A_{OCa} * \pi_{act,OCa}^{TGF\beta} * OCa \tag{3}$$

where, D_i are the differentiation rates of the cell 'i'; A_i the apoptosis rates and P_i the proliferation rates (see (Pivonka, Zimak et al. 2008) for details).

An important element in the remodeling process is the bone volume fraction: f_{bm}. It is the proportion of bone matrix in a volume of bone. Bone can be described as a two-phase material: the solid part, the matrix and the vascular part, the pores. With f_{vas} the proportion of pores we have:

$$f_{bm} = \frac{V_{bm}}{V_{total}} \qquad and \qquad f_{bm} + f_{vas} = 1 \tag{4 - 5}$$

(Martin 1972), in his work well explained how the porosity change during the remodeling process. The change in porosity is the difference between the total resorption of the osteoclasts and the total formation of the osteoblasts. And so, the changes of the bone matrix volume fraction over time can be represented by:

$$\frac{df_{bm}}{dt} = k_{form} * OB_a - k_{res} * OC_a \tag{6}$$

where k_{form} and k_{res} are the relative bone formation and resorption rates respectively. In a healthy (i.e., homeostatic) state, there is no change in the porosity/bone matrix volume fraction since the formation and the resorption are in equilibrium. In the following, this state will be referred to as the steady-state of the system.

The numerical simulation results are divided into two parts. The first part deals with simulations of the steady-state of the system which allows calculation of suitable initial conditions of uncommitted cell numbers and respective constants in the activator/repressor functions. The second set of simulations deal with age-related bone loss which is obtained by perturbing the initial healthy state. Based on this perturbation we can follow the temporal changes of cell numbers, regulatory factors and bone volume fractions.

Results and discussion

Changing the geometrical feedback

In the paper ref (Pivonka, Buenzli et al. 2013), the geometric regulation has been defined as in equation 1 where $S_{V\,to}$ is the specific surface for the steady state. This type of normalization of g_i leads to $g_i\,(t_0) = 1$. Hence, no recalibration of the original model was required for estimating steady-states of the system. Whereas this formulation seems suitable for discrete states of cortical and trabecular bone it is not clear how a continuous transition as in a spatio-temporal setting can be achieved with this formulation.

For these reasons, we renormalize by $S_{V\,to} = 1$ mm^{-1} in the current paper. We note that also in the model of Martin and others a similar approach has been applied. Introducing this normalization in Equation (1) would lead to changes in the differentiation rates. Indeed, $S_{V\,to}$ varies between 0 and 4 mm^{-1}.

In order to have the same differentiation rates as in previous models, we renormalize the various differentiation rates according to the following relationship:

$$D_i^{present\,model} * g_i = D_i^{previous\,model} \tag{8}$$

Calibration of the uncommitted cell populations: porosity dependence

Previously, OC$_u$ and OB$_u$ cell densities were considered constant and assumed to be large compared to the cell densities of the state-variables. Based on bone biology literature we take: $k_{res} = 9.425.10^{-6}mm^3/day$ and $k_{form} = 150\ \mu m^3/day$ (Buenzli, Pivonka et al. 2013).

Here, we assume OB$_u$ and OC$_u$ densities to be porosity dependent. We impose OC$_u$(f$_{bm}$), as a sigmoidal function of f$_{bm}$ in order to have approximately a 4 times change in the amplitude of OC$_u$ ($1.5*10^{-3} \leq OC_u \leq 5*10^{-3}$ pM). In the steady state, OB$_u$ density is unknown. Using the equilibrium constraint, i.e. resorption equals formation; we obtain 5 equations for the 5 unknowns. We are solving these equations using the Newton algorithm. By solving this problem at discrete porosities for the entire range (from 0 to 100%), we determine OB$_u$(f$_{bm}$) (see Figure 3a) at discrete points. These discrete values are then interpolated (using a linear interpolation) in order to obtain continuous functions of OB$_u$(f$_{bm}$) and OC$_u$(f$_{bm}$) which are then used for the subsequent dynamic simulations.
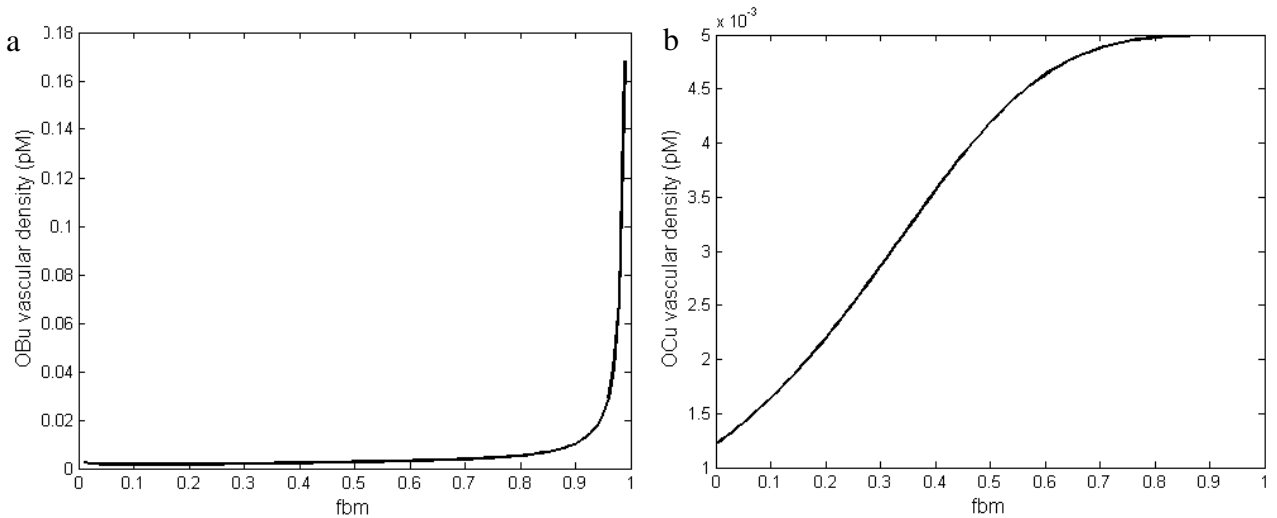

Figure 3 – Dependence of uncommitted bone cells on bone matrix volume fractions f$_{bm}$. (a) Uncommitted osteoblasts, (computed function) and (b) Uncommitted osteoclasts (imposed function)

The vascular density is the density inside the pores. This is why we assume this density to be higher where the porosity is low (i.e., $f_{bm} = 1$). Indeed, vascular pores in cortical bone are filled of blood vessels and BMUs. However, close to the marrow cavity, the trabecular pores are bigger but contains many other components. And so the density of bone cells in the vascular space is higher in cortical bone then in trabecular bone.

Calibration of the Hill functions
Due to the novel model features some of the previously defined Hill functions require recalibration. One of the most important Hill function is: $\pi_{act,OBu}^{TGF\beta}$, i.e., the TGFβ activator function which promotes differentiation of bone marrow stromal cells (OB$_u$s) into osteoblast precursor cells. Note that TGFβ is released from the bone matrix during osteoclastic resorption and provides a biochemical feedback on both osteoclastic and osteoblastic cells. The activator function is expressed as:

$$\pi_{act,OBu}^{TGF\beta} = \frac{\alpha.k_{res}.OC_a}{K_{rep} + \alpha.k_{res}.OC_a} \tag{9}$$

where α is a proportionality constant expressing the TGFβ content stored in the bone volume and K_{rep} is the dissociation constant. In the original model K_{rep} has been calibrated such as to obtain a strong biochemical feedback response. In order to test the suitability of the choice of K_{rep} in the current model we investigate the case of age-related bone loss. Similar as in previous models we induce age-related bone loss by increasing the PTH concentration. Osteoporosis is characterized by an increase in porosity. To simulate OP in our model, we perturb the homeostatic state by increasing the RANKL/OPG ratio. This can be achieved by prescribing an excess of PTH concentration. This increase in PTH leads to an increase in RANKL and a decrease in OPG leading to an overall increase in the RANKL/OPG ratio. This increase promotes osteoclastic resorption and, hence, an increase in the TGFβ concentration. To obtain an increase in porosity of about 2%/year as assumed by Buenzli (Buenzli, Thomas et al. 2013), a continuous injection of PTH has been applied: $P_{PTH}(t) = 15$ pM/day for all times $t > t_0$.

In Figure 4 we show the response of the TGFβ activator function for the case of age-related bone loss for different values of the dissociation constant (K_{rep}). The red parts of these plots represent the temporal changes of $\pi_{act,OBu}^{TGF\beta}$ over the simulation time ($t_0 = 0$, $t_{end} = 50$ years) while the black parts on the curves represent a larger interval of active osteoclast concentrations. Interestingly, we can see that use of the original value of K_{rep} (solid line) leads to an almost linear response of $\pi_{act,OBu}^{TGF\beta}$ with negligible changes in values. On the other hand, using $K_{rep} = 1.10^{-3}.K_{init}$ leads to a very strong non-linear response with values ranging between 0.40 and 0.77 for the investigated simulation time. Clearly the original K_{rep} value doesn't lead to a sensitive model response due to the introduced porosity dependent OB$_u$ and OC$_u$ values. Based on this parametric study we chose the $K_{rep} = 1.10^{-2}.K_{init}$ (dashed lines) which leads to an intermediate response with values changing from $0.16 - 0.41$.
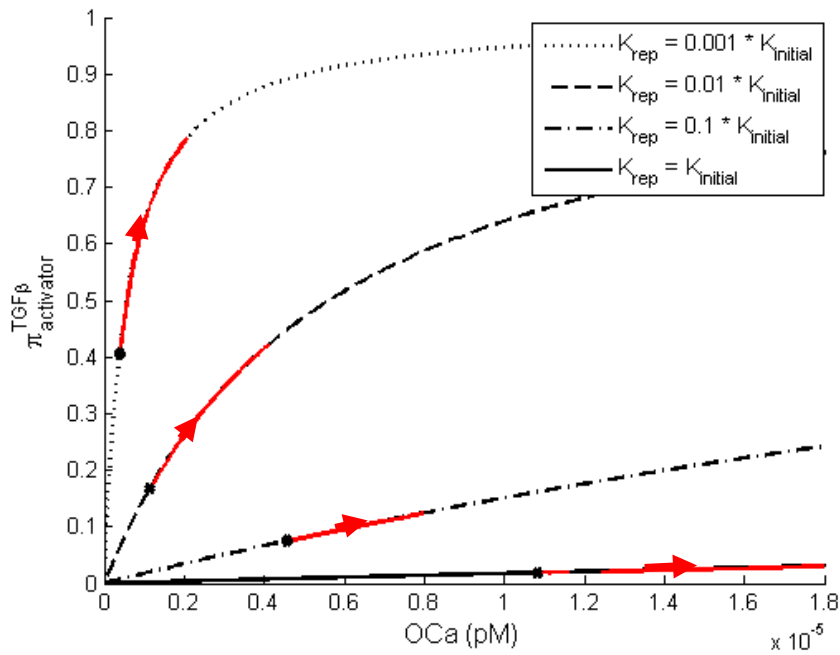
Figure 4 - Hill function for the regulation of TGF β depending on the active osteoclasts density. In red the portion of the curve where the osteoclasts density is in the model
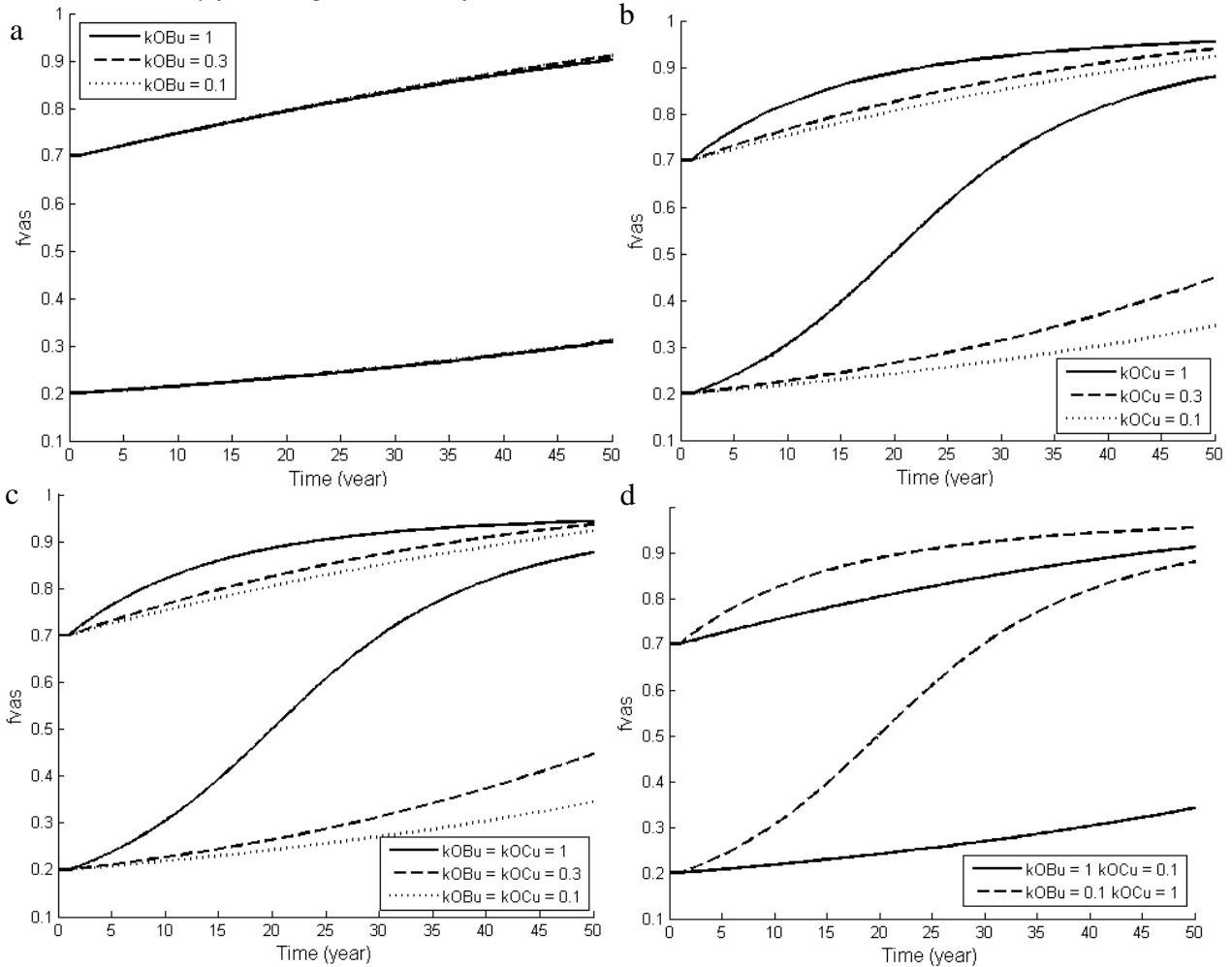
Parametric study for the geometrical feedback

Figure 5 - Parametric study showing the evolution of the porosity depending on the time for several regulatory functions: a) g_{OBu} b) g_{OCu} c) $g_{OBu} = g_{OCu}$ d) g_{OBu} and g_{OCu} differently regulated.

After having checked the suitability of the respective model parameters we are now in a position to study the effects of the different geometric regulatory functions $g_i(f_{bm})$, i.e., Eqn.(1) in more detail. In order to determine the effect of different choices of g_i with different values of k_i we apply a similar strategy as in (Pivonka, Buenzli et al. 2013). We tested: $k_i = 0$; 0.1; 0.3 and 1 on both uncommitted osteoblasts and osteoclasts with different combinations.

The objective of introducing a geometrical feedback in the model is to observe the acceleration of bone loss in trabecular bones and deceleration in cortical bones. This idea has been introduced by (Martin 1972) and was further explored in (Pivonka, Buenzli et al. 2013).
The graphs in Figure 5 show that the geometrical regulation needs to be preferentially on OC_u. For the case $k_{OCu} = 0$ (Figure 5a). no acceleration of cortical bone loss is observed. For all other combinations, the expected behavior is observed indicating that the suggested model is capable of representing geometrical feedback. In the following, we chose $k_{OBu} = k_{OCu} = 0.3$ as the combined regulation of both OB_u and OC_u, which leads to the anticipated geometrical behavior (Figure 5c). Indeed the other cases lead either to a too strong regulation ($k_{OCu} = 1$) or a not sufficiently strong regulation ($k_{OCu} = 0.1$).

Conclusions

Here we presented a consistent bone cell population model which takes into account bone specific surface on bone remodeling. Indeed, this model is able to simulate age-related bone loss for all different initial conditions of porosity. The results are in good qualitative and quantitative agreement with data reported in the literature.
As a next model development we will introduce a mechanical feedback and apply this coupled model to assess spatio-temporal changes in a cortical bone cross section. Using this methodology will help to better understand the experimentally observed phenomenon of trabecularization.

References

Buenzli, P. R., P. Pivonka, et al. (2013). Bone refilling in cortical basic multicellular units: insights into tetracycline double labelling from a computational model. *Biomechanics and Modeling in Mechanobiology*.
Buenzli, P. R., C. D. L. Thomas, et al. (2013). Endocortical bone loss in osteoporosis: The role of bone surface availability. *INTERNATIONAL JOURNAL FOR NUMERICAL METHODS IN BIOMEDICAL ENGINEERING*.
Lemaire, V., F. L. Tobin, et al. (2004). Modeling the interactions between osteoblast and osteoclast activities in bone remodeling. *Journal of Theoretical Biology* **229**(3): 293-309.
Martin, R. B. (1972). EFFECTS OF GEOMETRIC FEEDBACK IN DEVELOPMENT OF OSTEOPOROSIS. *Journal of Biomechanics* **5**(5): 447-&.
Martin, R. B. (1984). POROSITY AND SPECIFIC SURFACE OF BONE. *Critical Reviews in Biomedical Engineering* **10**(3): 179-222.
Martin, T. (2004). Paracrine regulation of osteoclast formation and activity: milestones in discovery. *Journal of Musculoskeleton Neuron Interact* **4**: 243-253.
Parfitt, A. M. (1994). OSTEONAL AND HEMI-OSTEONAL REMODELING - THE SPATIAL AND TEMPORAL FRAMEWORK FOR SIGNAL TRAFFIC IN ADULT HUMAN BONE. *J. C. B.* **55**(3): 273-286.
Pivonka, P., P. R. Buenzli, et al. (2013). The influence of bone surface availability in bone remodelling-A mathematical model including coupled geometrical and biomechanical regulations of bone cells. *Eng. Struct.* **47**: 134-147.
Pivonka, P., J. Zimak, et al. (2008). Model structure and control of bone remodeling: A theoretical study. *Bone* **43**(2): 249-263.
Pivonka, P., J. Zimak, et al. (2010). Theoretical investigation of the role of the RANK-RANKL-OPG system in bone remodeling. *Journal of Theoretical Biology* **262**(2): 306-316.
Roodman, G. D. (1999). Cell biology of the osteoclast. *Experimental Hematology* **27**(8): 1229-1241.
Scheiner, S., P. Pivonka, et al. (2013). Coupling systems biology with multiscale mechanics, for computer simulations of bone remodeling. *Computer Methods in Applied Mechanics and Engineering* **254**: 181-196.
CELLML website: http://models.cellml.org/exposure/51d04b5d2e2fe5abe8ac818a0c833b9c